Molecular Electronics

DOI: 10.1002/ange.200604398

Encoding Molecular-Wire Formation within Nanoscale Sockets**

Jinyao Tang, Yiliang Wang, Jennifer E. Klare, George S. Tulevski, Shalom J. Wind, and Colin Nuckolls**

Dedicated to Professor Julius Rebek, Jr.

We detail here a method to integrate chemical synthesis with the formation of nanoscale electrical "sockets" to allow the in situ construction of three-component molecular wires. Reaction chemistry offers molecular materials an overwhelming amount of diversity and functionality and could provide a method for nanoscale electronics to be synthesized rather than fabricated.[1] Though presently underutilized, this approach can be used to produce multifaceted electrical components on the molecular scale by a combination of self-assembly and programmed reactivity. This approach contrasts with previous work in molecular electronics, which has typically relied on ex situ synthesis[2–5] of wire components followed by their subsequent insertion into devices.[6–20] The wires typically used in this context are dithiolated aromatics or other bifunctionalized molecules, which are intended to bridge from one electrode surface to another.[2,3,5,21–24] One complication associated with dithiols is their tendency to undergo oxidative oligomerization, which allows them to span gaps much longer than an individual molecule.[25] In addition, these molecules can orient both of their surface-active groups toward the same electrode.[4,26,27]

The present study circumvents these problems through the implementation of a two-step reaction sequence between molecular-scale electrodes: first, we assemble a bifunctional molecule into a monolayer on the electrode surface, such that only one end of the molecule reacts with the electrode; then, we use a second molecule to bridge the gap between the termini of the films (Figure 1a).

The two reaction sequences explored in this study are shown in Figure 1b,c. In both cases, a metal surface is reacted with a monothiolated aromatic compound to form a monolayer.[28–31] We chose platinum as the electrode material because the film is metallic despite being only a few atoms thick on the surface of zirconium oxide.[32] We chose thiols because they are known to readily form strong bonds with platinum surfaces.[29,30,33] For the monolayers that are terminated with terpyridyl units, we chose transition-metal ions to connect the two ends through well-known coordination chemistry (Figure 1b).[34,35] Cobalt ions, in particular, are attractive because their complexes are readily formed at room temperature with a variety of terpyridyl ligands.[35] We also studied aldehyde-terminated bisoxazole monolayers and their reactions with aromatic amines (Figure 1c).[24] This reaction is advantageous because it provides a system that is conjugated across the entire length of the molecular bridge.

We performed model studies on large-area, planar metal surfaces to assess the feasibility of these linking reactions by first preparing monolayers and then reacting them with the bridging subunits (shown in Figure 2a,b). The reaction between the aldehyde-terminated monolayers **1** and the amine-functionalized aromatics to give **2** (Figure 2a) readily occur and are described elsewhere.[24] The other reaction we investigated is that between the terpyridyl-terminated monolayer **3** and a solution of cobalt(II) diacetate. Using X-ray photoelectron spectroscopy (XPS), we found that that the coverage of both monolayers, **1** and **3**, is quantitative and that the layer heights ($\approx$2.3 nm and $\approx$1.4 nm, respectively) are consistent with an upright orientation of the molecule.[36] Figure 2c shows the XPS spectra from the cobalt and carbon regions from monolayer **3** as it is reacted with $Co(OAc)_2$. We observed transitions for the Co $2p_{3/2}$ (781 eV) and Co $2p_{1/2}$ (797 eV) energy levels, which are indicative of a cobalt(II) species bound to the surface.[37] In addition, we observed the smaller satellite peaks (786 and 803 eV) indicative of the formation of cobalt hydroxide or oxidized cobalt species.[37] In the carbon (C1s) region of the XPS spectrum after reaction, a new peak characteristic of the

[*] Dr. S. J. Wind
Department of Applied Physics/Applied Mathematics and
The Center for Electron Transport in Molecular Nanostructures
Columbia University
New York, NY 10027 (USA)
Fax: (+1) 212-854-1909
E-mail: sw2128@columbia.edu
Homepage: http://nuckolls.chem.columbia.edu

J. Tang, Y. Wang, J. E. Klare, G. S. Tulevski, Prof. C. Nuckolls
Department of Chemistry and
The Center for Electron Transport in Molecular Nanostructures
Columbia University
New York, NY 10027 (USA)
Fax: (+1) 212-932-1289
E-mail: cn37@columbia.edu

[**] We are grateful to Cherie Kagan, Michael Steigerwald, and Horst Stormer for enlightening discussions. We acknowledge financial support from the Nanoscale Science and Engineering Initiative of the National Science Foundation (NSF Award Number CHE-0117752), the New York State Office of Science, Technology, and Academic Research (NYSTAR), and the Chemical Sciences, Geosciences, and Biosciences Division, Office of Basic Energy Sciences, US Department of Energy (DE-FG02-01ER15264). J.E.K. thanks the American Chemical Society Division of Organic Chemistry sponsored by Organic Syntheses for a fellowship. G.S.T. is grateful for an Arun Guthikonda Memorial Fellowship.

Supporting information for this article (experimental details for the molecular synthesis, monolayer characterization, junction fabrication, electrical testing, and current voltage curves for the control experiments) is available on the WWW under http://www.angewandte.org or from the author.

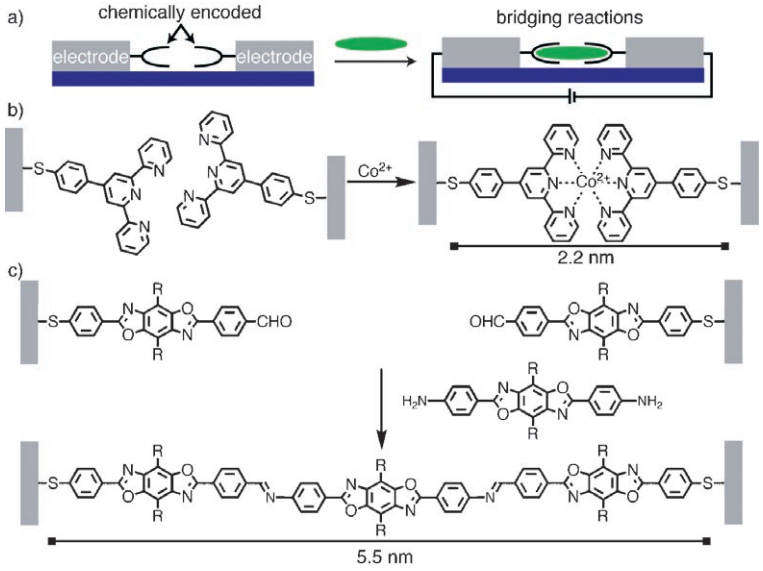

Figure 1. a) Two-step sequence to bridge electrode surfaces. b) Bridging by first forming a monolayer with the terpyridyl group and using cobalt ions to orchestrate wire formation. c) Bridging gaps by first forming a thiol-terminated monolayer and then reacting with a diamine. The R group is a 4-dodecyloxy-substituted phenyl group added to improve solubility.

that both the aldehyde-terminated and the terpyridyl-terminated monolayers are able to serve as a priming monolayer to react with a bridging component.

Next, we explored the reversibility of the reaction with cobalt ions in the terpyridyl monolayers. We used solutions of EDTA to react with the monolayers of **4** and found that the IR and XPS spectroscopic signatures for the cobalt ions and their associated counterions disappeared (shown in Figure 2c). The carbons indicative of the backbone were still present, indicating that the monolayer is intact and able to once again bind cobalt ions. These studies indicate that the terpyridyl ligands on the surface are able to bind and release their ions without desorbing.

To test these reactions within molecular electronic devices, we created a new technique to fabricate molecular-scale electrical test structures (Figure 3).[39,40] The key advantage of this technique is that it is a self-aligned lithographic process able to produce large numbers of molecular-scale gaps with remarkably high yield and precision.

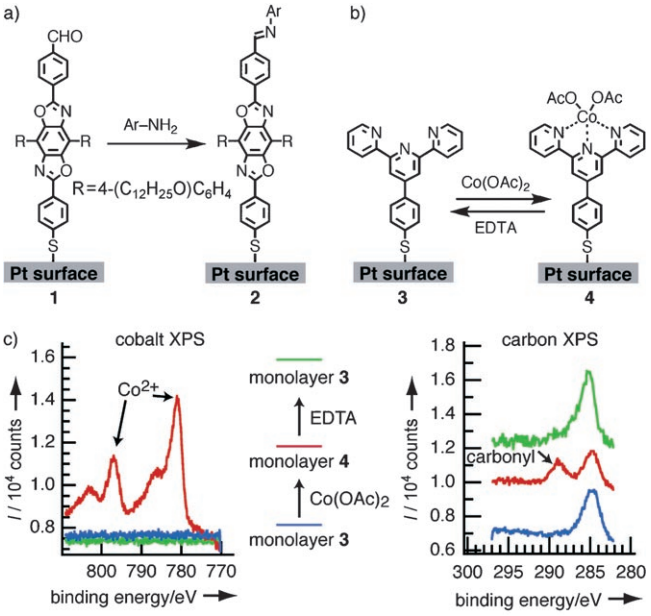

Figure 2. a) Aldehyde-terminated monolayers react with diamines to form imine linkages. b) Terpyridyl-terminated monolayers form linkages from cobalt diacetate. c) XPS analysis of the cobalt and carbon regions of the spectrum for terpyridyl-terminated monolayers (blue line), reacted with $Co(OAc)_2$ solutions (red line), and then returned to the metal-free state (green line) by reaction with a solution of ethylenediaminetetraacetic acid (EDTA).

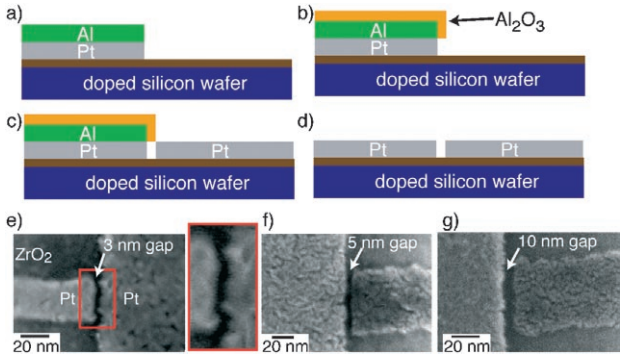

Figure 3. a) A line of Al on Pt is patterned by electron-beam lithography on a silicon wafer coated with ZrO_2. b) Oxygen in the ambient oxidizes aluminum to produce an overhanging aluminum oxide layer. c) Evaporation of the counter electrode produces platinum separated by the amount of aluminum oxide overhang. d) Dissolving the aluminum/aluminum oxide layer give closely spaced platinum electrodes. e) Scanning electron micrograph (SEM) showing a 3-nm gap; the part in the red rectangle is enlarged by 200% and shown to the right. f) SEM showing a 5-nm gap. g) SEM showing a 10-nm gap.

carbonyl in the acetate counterion emerges at approximately 289 eV (Figure 2c).[26] We also detected the acetate counterion with reflection absorption infrared spectroscopy (RAIRS) from a new resonance indicative of a carbonyl group at 1724 cm^{-1}.[38] From these spectroscopic studies, we conclude

First, we deposited 5 nm of ZrO_2 by atomic-layer deposition (ALD) onto a clean silicon wafer (20 nm thermal SiO_2). We defined the first electrode ($\approx$200-nm wide) with electron-beam lithography (the beam resist is 150-nm thick, 25 kDa polymethyl methacrylate (PMMA)). Then, we deposited 3 nm Pt and 2.5–7 nm Al (Figure 3a) by electron-beam evaporation at a pressure of about 1×10^{-6} Torr. To obtain the narrowest gaps, 5 nm of SiO_2 was added between the platinum and the aluminum films to aid the subsequent removal of the thin Al film. Upon exposure to ambient oxygen, a thin native oxide layer formed on the aluminum surface; the oxide on the edge of the Al film formed an

overhang structure over the Pt electrode after lift-off (Figure 3b). The second electrode, around 30-nm wide, consisted of 2.5 nm Pt defined by electron-beam lithography overlapping with the first electrode (Figure 3c). The overlapping part of the second electrode, along with the oxidized aluminum, was removed in 0.22 M tetramethylammonium hydroxide solution to form the nanosized gaps (Figure 3d).

Figure 3e–g shows nanosized gaps of approximately 3, 5, and 10 nm prepared by this method. The gap between the electrodes is determined by the thickness of the aluminum oxide layer, which scales with the thickness of the aluminum film for these ultrathin films. An interesting feature of this self-aligned lithographic process is that the overall shape and curvature of one electrode is mirrored by the counter electrode (shown in the enlargement of the gap region in Figure 3e). The protrusions on one electrode create depressions in the counter electrode, while maintaining the gap size along the length of the electrode. This technique addresses one of the problems associated with extremely small electrode spacings where defects and irregularities can fill the gap to produce lower yields and complicate the interpretation of the electrical measurements.[41,42]

Next, we combined these nanoscale electrodes with the bridging chemistry developed above. After cleaning the electrodes with water and alcohol, we primed the surface with the monolayer-forming molecules that are terminated with either terpyridyls or aldehydes. There was essentially no change in the electrical properties of the devices after reaction with these thiols (shown in Figure 4a,b). Reactions of these primed electrode surfaces with the bridging molecules turned the devices to the ON state (Figure 4a,b). The yield for working devices was 27% (32 out of 120 electrode pairs) for the reaction of cobalt acetate with the electrodes primed with the terpyridyl groups, and was 13% (8 out of 60 electrode pairs) for the reaction of the diamines with the electrodes primed with aldehydes. These yields are based on devices that before connection are at the noise level of the measurement ($\approx$10 pA) and after connection show currents that are greater than 1 nA at 2 V bias. For the terpyridyl devices, the range of currents (at 2 V bias) for the working devices was between 7–50 nA. The higher yield for the junctions formed through coordination chemistry may reflect a greater degree of reversibility and less restrictive bonding angles relative to imine bridges.

In general, the devices that are bridged with imines show higher current levels despite being 3.3 nm longer than the cobalt complexes. The area of the electrode surface ($\approx$60 nm^2) determines how many molecular bridges can form and allows us to estimate upper and lower limits on the conductance of an individual molecular wire. As was shown above, the self-assembled monolayers of both the aldehyde-terminated films and the terpyridyl-terminated monolayers have high coverage and are upright. In the case of the aldehyde-terminated monolayers, about 23 molecules would cover the entire lateral edge of the electrode. If somewhere between one and 23 parallel imine bridges form, then the conductance (from the data in Figure 4a) for each metal–wire–metal junction would range between 1×10^{-3} and 5×10^{-5} e^2h^{-1}.[43] Similarly, for the cobalt terpyridyl wires, the conductance for each wire would be between 1.3×10^{-4} and 1.6×10^{-6} e^2h^{-1} for 1–80 molecular bridges. The origin of the higher conductance of the imine bridges is likely the result of better π-orbital overlap through the molecule relative to the tetrahedral coordination of the cobalt terpyridyl complex.

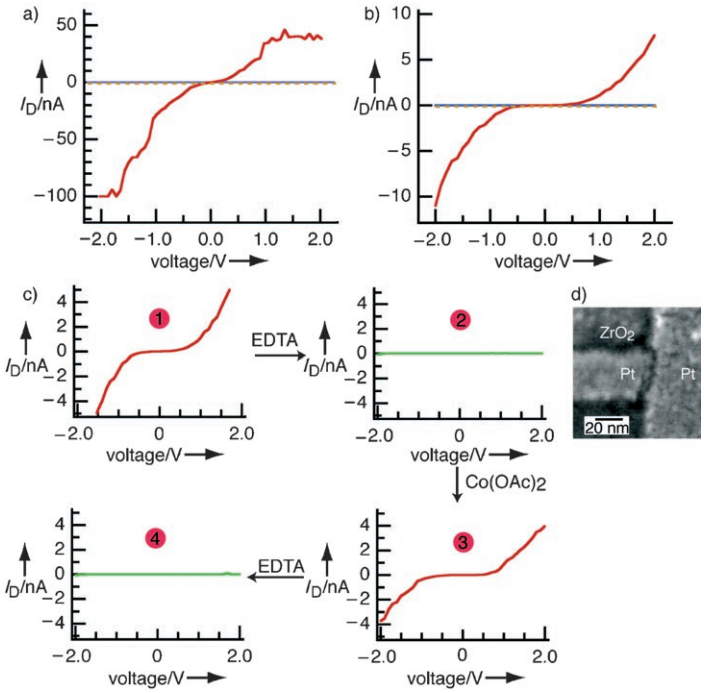

Figure 4. a) Reaction sequence showing the current versus voltage curves for the unreacted device (blue trace at $I_D\approx0$), the device after monolayer formation with the aldehyde-terminated thiol **1** (dashed yellow trace at $I_D\approx0$), and after reaction with the diamine bridge (red trace). b) Reaction sequence showing the current versus voltage curves for the unreacted device (blue trace at $I_D\approx0$), the device after monolayer formation with the terpyridyl-terminated thiol **3** (dashed yellow trace at $I_D\approx0$), and after reaction with cobalt diacetate (red trace). c) The device from part (b) (1) after reaction with EDTA to strip out the metal bridge (2), after reinsertion of the metal ion (3), and after re-removal of the metal ion (4). d) SEM of the device used in part (c) after the reaction sequence.

The coordination complexes offer the chance to study the reversibility of these reactions. Figure 4c shows a cycle of decomplexation and complexation with cobalt ions for the same device shown in Figure 4b. After we immerse the connected device in a solution of EDTA, it returns to an open circuit. Once again, when we introduce $Co(OAc)_2$, the device returns to the ON state. We can again switch the device to the OFF state by treatment with EDTA.

We performed several control experiments based on the results presented above. When the order of the steps was reversed (i.e. when the junction was "reacted" with the bridging molecule first and then the monolayer-forming molecule), there were no connected devices (Figure S1 in the Supporting Information). When 8-nm gaps were utilized, which are too large for the cobalt terpyridyl complex to bridge, we measured current at the noise level of the

measurement in about 120 devices (Figure S2 in the Supporting Information). When we first used the monolayer that is terminated with terpyridyls and then added the diamine bridge, we observed no connected devices (Figure S3 in the Supporting Information). Similarly, if we used the aldehyde-terminated monolayer or an unfunctionalized terphenylthiol and introduced cobalt ions, we observed no increase in current (Figure S4 in the Supporting Information). These "mismatched" control experiments are important because they show that the junctions, once derivatized, are able to display orthogonal recognition. This type of mutual exclusivity could be used to spatially address and construct complex molecular circuits. Finally, if we form dithiol ex situ from the complex between the terpyridyl and the cobalt ions, the yield of working devices is very low ($\approx 2\%$ yield). The reason for the low yield may be as a result of steric effects, which prevent upright packing in the preformed complexes.

In summary, we have detailed above a method to prepare multicomponent electrical circuits through the nanoscale placement of reactive groups. This approach is useful because it not only circumvents the assembly and reactivity problems associated with dithiols but also provides a method by which complex materials can be made and measured and provides a clear path to multifunctional molecular electronic materials.

Received: October 27, 2006
Published online: March 7, 2007

Keywords: molecular electronics · monolayers · nanotechnology · self-assembly · transition metals

[1] C. Lin, C. R. Kagan, *J. Am. Chem. Soc.* **2003**, *125*, 336.
[2] J. M. Tour, *Acc. Chem. Res.* **2000**, *33*, 791.
[3] N. Robertson, C. A. McGowan, *Chem. Soc. Rev.* **2003**, *32*, 96.
[4] B. de Boer, H. Meng, D. F. Perepichka, J. Zheng, M. M. Frank, Y. J. Chabal, Z. Bao, *Langmuir* **2003**, *19*, 4272.
[5] J. E. Klare, G. S. Tulevski, K. Sugo, A. de Picciotto, K. A. White, C. Nuckolls, *J. Am. Chem. Soc.* **2003**, *125*, 6030.
[6] M. A. Reed, C. Zhou, C. J. Muller, T. P. Burgin, J. M. Tour, *Science* **1997**, *278*, 252.
[7] J. Chen, M. A. Reed, A. M. Rawlett, J. M. Tour, *Science* **1999**, *286*, 1550.
[8] W. Liang, M. P. Shores, M. Bockrath, J. R. Long, H. Park, *Nature* **2002**, *417*, 725.
[9] J. G. Kushmerick, D. B. Holt, S. K. Pollack, M. A. Ratner, J. C. Yang, T. L. Schull, J. Naciri, M. H. Moore, R. Shashidhar, *J. Am. Chem. Soc.* **2002**, *124*, 10654.
[10] J. Park, A. N. Pasupathy, J. I. Goldsmith, C. Chang, Y. Yaish, J. R. Petta, M. Rinkoski, J. P. Sethna, H. D. Abruna, P. L. McEuen, D. C. Ralph, *Nature* **2002**, *417*, 722.
[11] N. B. Zhitenev, H. Meng, Z. Bao, *Phys. Rev. Lett.* **2002**, *88*, 226801.
[12] M. A. Rampi, G. M. Whitesides, *Chem. Phys.* **2002**, *281*, 373.
[13] J. K. N. Mbindyo, T. E. Mallouk, J. B. Mattzela, I. Kratochvilova, B. Razavi, T. N. Jackson, T. S. Mayer, *J. Am. Chem. Soc.* **2002**, *124*, 4020.
[14] M. Mayor, H. B. Weber, J. Reichert, M. Elbing, C. von Haenisch, D. Beckmann, M. Fischer, *Angew. Chem.* **2003**, *115*, 6014; *Angew. Chem. Int. Ed.* **2003**, *42*, 5834.
[15] N. B. Zhitenev, A. Erbe, Z. Bao, *Phys. Rev. Lett.* **2004**, *92*, 186805.
[16] L. T. Cai, H. Skulason, J. G. Kushmerick, S. K. Pollack, J. Naciri, R. Shashidhar, D. L. Allara, T. E. Mallouk, T. S. Mayer, *J. Phys. Chem. B* **2004**, *108*, 2827.
[17] M. Elbing, R. Ochs, M. Koentopp, M. Fischer, C. von Haenisch, F. Weigend, F. Evers, H. B. Weber, M. Mayor, *Proc. Natl. Acad. Sci. USA* **2005**, *102*, 8815.
[18] X. Li, J. He, J. Hihath, B. Xu, S. M. Lindsay, N. Tao, *J. Am. Chem. Soc.* **2006**, *128*, 2135.
[19] L. Venkataraman, J. E. Klare, I. W. Tam, C. Nuckolls, M. S. Hybertsen, M. L. Steigerwald, *Nano Lett.* **2006**, *6*, 458.
[20] X. Guo, J. P. Small, J. E. Klare, Y. Wang, M. S. Purewal, I. W. Tam, B. H. Hong, R. Caldwell, L. Huang, S. O'Brien, J. Yan, R. Breslow, S. J. Wind, J. Hone, P. Kim, C. Nuckolls, *Science* **2006**, *311*, 356.
[21] J. I. Henderson, S. Feng, T. Bein, C. P. Kubiak, *Langmuir* **2000**, *16*, 6183.
[22] D. Cahen, G. Hodes, *Adv. Mater.* **2002**, *14*, 789.
[23] D. K. James, J. M. Tour, *Chem. Mater.* **2004**, *16*, 4423.
[24] J. E. Klare, G. S. Tulevski, C. Nuckolls, *Langmuir* **2004**, *20*, 10068.
[25] J. M. Tour, L. Jones, II, D. L. Pearson, J. J. S. Lamba, T. P. Burgin, G. M. Whitesides, D. L. Allara, A. N. Parikh, S. Atre, *J. Am. Chem. Soc.* **1995**, *117*, 9529.
[26] C. D. Bain, E. B. Troughton, Y. T. Tao, J. Evall, G. M. Whitesides, R. G. Nuzzo, *J. Am. Chem. Soc.* **1989**, *111*, 321.
[27] L. Pranger, A. Goldstein, R. Tannenbaum, *Langmuir* **2005**, *21*, 5396.
[28] C. M. Bell, S. W. Keller, V. M. Lynch, T. E. Mallouk, *Mater. Chem. Phys.* **1993**, *35*, 225.
[29] A. Ulman, *Chem. Rev.* **1996**, *96*, 1533.
[30] F. Schreiber, *Prog. Surf. Sci.* **2000**, *65*, 151.
[31] A. Ulman, *Acc. Chem. Res.* **2001**, *34*, 855.
[32] E. P. De Poortere, H. L. Stormer, L. M. Huang, S. J. Wind, S. O'Brien, M. Huang, J. Hone, *Appl. Phys. Lett.* **2006**, *88*, 143124.
[33] G. M. Whitesides, J. K. Kriebel, J. C. Love, *Sci. Prog.* **2005**, *88*, 17.
[34] K. T. Potts, D. A. Usifer, A. Guadalupe, H. D. Abruna, *J. Am. Chem. Soc.* **1987**, *109*, 3961.
[35] M. Maskus, H. D. Abruna, *Langmuir* **1996**, *12*, 4455.
[36] By the method of C. D. Bain, G. M. J. Whitesides, *J. Phys. Chem.* **1989**, *93*, 1670.
[37] Z. Kónya, J. Kiss, A. Oszko, A. Siska, I. Kiricsi, *Phys. Chem. Chem. Phys.* **2001**, *3*, 155.
[38] K. Nakanishi, P. H. Solomon, *Infrared Absorption Spectroscopy*, Holden-Day, San Francisco, **1977**.
[39] J. Tang, E. P. De Poortere, J. E. Klare, C. Nuckolls, S. J. Wind, *Microelectron. Eng.* **2006**, *83*, 1706.
[40] This method, while similar to the angle evaporation techniques previously described (e.g. E. T. T. Jones, O. M. Chyan, and M. S. Wrighton, *J. Am. Chem. Soc.* **1987**, *109*, 5526), offers smaller electrode spacings and greater reproducibility. It also avoids the low yields at nanoscale electrode separations that are a consequence of the grain structure of the metal (L. F. Sun, S. N. Chin, E. Marx, K. S. Curtis, N. C. Greenham, C. J. B. Ford, *Nanotechnology* **2005**, *16*, 631).
[41] A. de Picciotto, J. E. Klare, C. Nuckolls, K. Baldwin, A. Erbe, R. Willett, *Nanotechnology* **2005**, *16*, 3110.
[42] A. A. Houck, J. Labaziewicz, E. K. Chan, J. A. Folk, I. L. Chuang, *Nano Lett.* **2005**, *5*, 1685.
[43] The units used in this study are derived from the fundamental quantum of conductance. The values obtained for these molecular wires are consistent with values for other similar molecular wires: see reference [19].

